JCB Report

Cell cycle– and swelling-induced activation of a *Caenorhabditis elegans* ClC channel is mediated by CeGLC-7α/β phosphatases

Eric Rutledge,[1] Jerod Denton,[1] and Kevin Strange[1,2,3]

[1]Department of Anesthesiology, [2]Department of Molecular Physiology, and [3]Department of Biophysics and Pharmacology, Vanderbilt University Medical Center, Nashville, TN 37232

ClC voltage-gated anion channels have been identified in bacteria, yeast, plants, and animals. The biophysical and structural properties of ClCs have been studied extensively, but relatively little is known about their precise physiological functions. Furthermore, virtually nothing is known about the signaling pathways and molecular mechanisms that regulate channel activity. The nematode *Caenorhabditis elegans* provides significant experimental advantages for characterizing ion channel function and regulation. We have shown previously that the ClC Cl^- channel homologue CLH-3 is expressed in *C. elegans* oocytes, and that it is activated during meiotic maturation and by cell swelling. We demonstrate here that depletion of intracellular ATP or removal of Mg^{2+}, experimental maneuvers that inhibit kinase function, constitutively activate CLH-3. Maturation- and swelling-induced channel activation are inhibited by type 1 serine/threonine phosphatase inhibitors. RNA interference studies demonstrated that the type 1 protein phosphatases CeGLC-7α and β, both of which play essential regulatory roles in mitotic and meiotic cell cycle events, mediate CLH-3 activation. We have suggested previously that CLH-3 and mammalian ClC-2 are orthologues that play important roles in heterologous cell–cell interactions, intercellular communication, and regulation of cell cycle–dependent physiological processes. Consistent with this hypothesis, we show that heterologously expressed rat ClC-2 is also activated by serine/threonine dephosphorylation, suggesting that the two channels have common regulatory mechanisms.

Introduction

Anion channels play central roles in diverse physiological processes, such as intracellular vesicle acidification, cell cycle progression, control of cell excitability, cell volume regulation, epithelial salt and water transport, and programmed cell death (Frings et al., 2000; Gulbins et al., 2000; Wondergem et al., 2001; Jentsch et al., 2002). To date, four anion channel–encoding gene families have been identified unequivocally. These families include ligand-gated, ClC, CFTR, and VDAC anion channels. ClC channel–encoding genes have been found in plants, yeast, bacteria, and invertebrate and vertebrate animals. Knockout studies and identification of disease-causing mutations indicate that some ClC channels play roles in transepithelial Cl^- transport, Cl^- transport in intracellular vesicles, and regulation of membrane potential (George et al., 2001; Jentsch et al., 2002).

The biophysical and structural properties of ClC channels have been studied extensively (Maduke et al., 2000; Dutzler et al., 2002; Jentsch et al., 2002). However, detailed understanding of the precise physiological functions of most ClC channels is lacking. In addition, virtually nothing is known about the signaling pathways and molecular mechanisms that regulate channel activity. The nematode *Caenorhabditis elegans* provides significant experimental advantages for characterizing ion channel integrative physiology and for defining the molecular bases of channel regulation. These advantages include a fully sequenced genome, a short life cycle, genetic tractability, and the relative ease and economy of manipulating gene function. Six ClC genes termed Cl^- channel homologue (*clh*)*-*1-6* (Petalcorin et al., 1999; Nehrke et al., 2000) or *CeClC-1-6* (Schriever et al., 1999) are present in the nematode genome.

Address correspondence to Dr. Kevin Strange, Vanderbilt University Medical Center, T-4202 Medical Center North, Nashville, TN 37232-2520. Tel.: (615) 343-7425. Fax: (615) 343-3916.
E-mail: kevin.strange@mcmail.vanderbilt.edu

Key words: chloride channel; meiosis; cell volume; oocyte; phosphorylation

*Abbreviations used in this paper: CA, calyculin A; CDK, cyclin-dependent kinase; CLH, Cl^- channel homologue; DIC, differential interference contrast; dsRNA, double-stranded RNA; NEBD, nuclear envelope breakdown; OA, okadaic acid; PP, protein phosphatase; RNA_i, RNA interference; RPE, retinal pigment epithelium.

© The Rockefeller University Press, 0021-9525/2002/08/435/10 $5.00

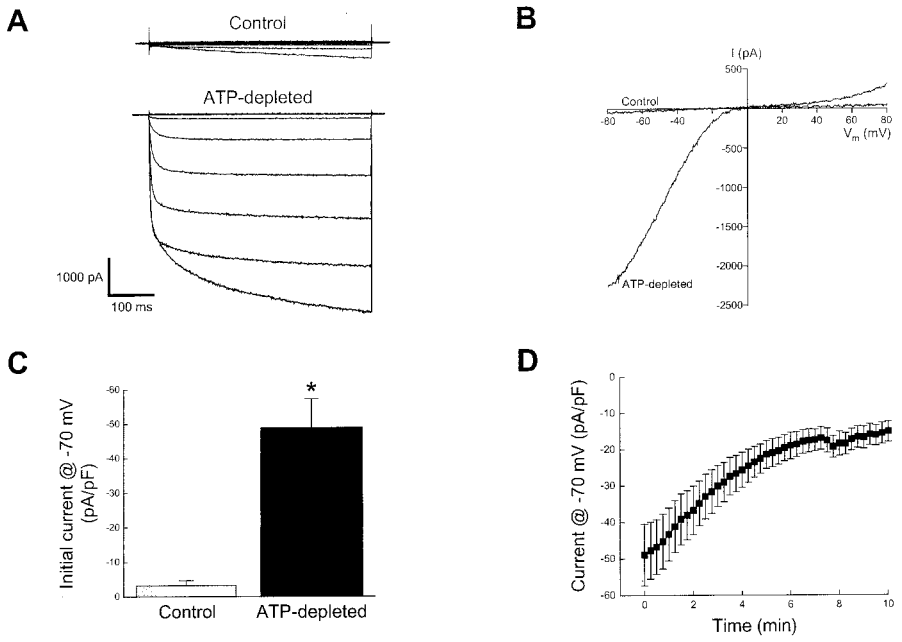

Figure 1. **Incubation of oocytes with metabolic inhibitors activates CLH-3.** (A) Whole-cell Cl^- currents observed immediately after membrane rupture in a nonmetabolically poisoned (Control) and an ATP-depleted oocyte incubated for 20–30 min with 5 mM 2-deoxyglucose and 1 μM rotenone. Currents were elicited by stepping membrane voltage from −120 mV to +80 mV in 20 mV steps from a holding potential of 0 mV. Under control conditions, strong (>−100 mV) hyperpolarization activates a small inwardly rectifying current. This current is inhibited >80% by *clh-3* dsRNA (Rutledge et al., 2001) and 70 ± 5% (−120 mV; $n = 3$) by 10 mM Zn^{2+} indicating that it is due to a small basal activity of CLH-3. (B) Current-to-voltage relationships of whole-cell Cl^- currents observed immediately after membrane rupture in ATP-depleted and control oocytes. Control oocytes were incubated in egg buffer containing 5 mM glucose and 0.01% DMSO for 20–30 min before they were patch clamped. Currents were elicited by ramping membrane potential from –80 mV to +80 mV at 80 mV/s. (C) Mean ± SE initial whole-cell Cl^- current densities in control ($n = 3$) and ATP-depleted ($n = 7$) oocytes. *$P < 0.002$ compared with control oocytes. (D) Time course of whole-cell current change in ATP-depleted oocytes. Time zero is defined as the time at which whole-cell access was obtained. Values are means ± SE ($n = 5$–7).

We demonstrated recently that *C. elegans* oocytes express a ClC channel encoded by *clh-3* (Rutledge et al., 2001). CLH-3 is activated during oocyte meiotic cell cycle progression, a process termed meiotic maturation, and in response to oocyte swelling. Knockdown of *clh-3* expression by RNA-mediated gene interference (RNA_i) disrupts the timing of ovulatory contractions of smooth muscle-like gonadal sheath cells (Rutledge et al., 2001). Ovulatory sheath cell contractions are initiated during meiotic maturation of oocytes (McCarter et al., 1999). Sheath cells surround oocytes and are coupled to them via gap junctions (Hall et al., 1999). We have suggested that activation of CLH-3 during meiotic maturation depolarizes the oocyte and electrically coupled sheath cells and that depolarization in turn modulates Ca^{2+} signaling pathways that control sheath contractility (Rutledge et al., 2001; Strange, 2002).

Patch clamp studies on nematode oocytes demonstrated that the volume sensitivity, voltage-dependent gating, anion selectivity, pharmacology, and extracellular pH sensitivity of CLH-3 are virtually identical to those of heterologously expressed mammalian ClC-2, as well as native ClC-2–like anion currents (Rutledge et al., 2001; Strange, 2002). Mammalian ClC-2 is expressed widely and is activated by membrane hyperpolarization and cell swelling. The functions of this channel are unknown, but it has been proposed to play roles in transepithelial Cl^- transport, intracellular Cl^- regulation, and cell volume homeostasis (George et al., 2001; Jentsch et al., 2002).

Bösl et al. (2001) reported recently that knockout of ClC-2 in mice causes progressive degeneration of the testes and retina. The mammalian seminiferous tubule is comprised of Sertoli cells and developing sperm cells that interact physically and functionally with each other. Similarly, photoreceptor cells in the retina are in intimate contact with and functionally dependent on the retinal pigment epithelium (RPE) (for review see Strange, 2002). The degeneration of the testes and retina in ClC-2 knockout mice suggested to Bösl et al. (2001) that the channel may regulate local ionic environments in tissues comprised of heterologous cell types that interact functionally with one another. Interestingly, nematode gonadal sheath cells and oocytes are coupled via gap junctions and functional interactions and signaling between the two cell types is essential for regulating oocyte development, meiotic cell cycle events, and ovulation (Greenstein et al., 1994; Rose et al., 1997; Hall et al., 1999; McCarter et al., 1999).

We have proposed that CLH-3 and ClC-2 are orthologues that carry out analogous physiological functions (Rutledge et al., 2001; Strange, 2002). Here we report that CLH-3 activation during oocyte meiotic cell cycle progression and in response to oocyte swelling is regulated by serine/threonine dephosphorylation. RNA_i studies demonstrate that dephosphorylation is mediated by the type 1 protein phosphatases CeGLC-7α and β. These two phosphatases have recently been shown to play important roles in controlling *C. elegans* meiotic and mitotic cell cycle events (Hsu et al., 2000; Kaitna et al., 2002; Rogers et al., 2002). We also demonstrate that heterologously expressed rat ClC-2 is activated by serine/threonine dephosphorylation, suggesting that CLH-3 and ClC-2 have common regulatory mechanisms. These results as well as recent studies on phosphorylation-dependent regulation of rabbit ClC-2 (Furukawa et al., 2002) further support the hypothesis that the two channels are orthologues that may play important roles in heterologous cell–cell interactions, intercellular communication, and regulation of cell cycle–dependent physiological processes.

Results

Kinase inhibition activates CLH-3

Meiotic and mitotic cell cycle progression are regulated critically by cycles of protein phosphorylation and dephosphorylation (Morgan, 1997; Berndt, 1999; Ferrell, 1999). Activation of CLH-3 at the beginning of meiotic maturation in the *C. elegans* oocyte (Rutledge et al., 2001) suggested that the channel might be regulated by phosphorylation/dephosphorylation events. To begin testing this hypothesis, we depleted oocytes of ATP by exposing them to 5 mM 2-deoxyglucose (2-DG) and 1 μM rotenone in egg buffer. After incubating for 20–30 min, oocytes were transferred to NMDG-Cl bath solution containing 2-DG and rotenone and patch clamped in the whole-cell configuration using an ATP-free pipette solution containing 40 μM oligomycin, 20 μM rotenone, and 5 μM iodoacetate. As shown in Fig. 1, A and B, a strongly inwardly rectifying Cl^- current was constitutively active in metabolically poisoned oocytes. Mean ± SE initial whole-cell Cl^- current densities observed immediately after obtaining whole-cell access in control and ATP-depleted oocytes were –3.2 ± 1.4 and –49 ± 8 pA/pF (n = 5–7) at –70 mV, respectively (Fig. 1 C). Whole-cell Cl^- current was significantly ($P < 0.002$) higher in metabolically poisoned oocytes.

Chloride currents in oocytes metabolically poisoned for 20–30 min were not stable and inactivated slowly after whole-cell access was obtained (Fig. 1 D). To determine if this rundown was due to prolonged metabolic inhibition, we exposed oocytes to 2-DG and rotenone for 60–70 min before performing patch clamp measurements. Under these conditions, the mean ± SE initial current density at –70 mV was –78 ± 24 pA/pF (n = 3), a value that is not significantly ($P > 0.2$) different from that observed with shorter periods of metabolic inhibition. A pattern of current inactivation similar to that shown in Fig. 1 D was observed within 1 to 2 min of obtaining whole-cell access on these oocytes (unpublished data). Preliminary cell-attached patch clamp studies have suggested that channel activity is stable in metabolically poisoned oocytes (unpublished data). Taken together, these results suggest that current inactivation during metabolic inhibition is likely a consequence of whole-cell patch clamping rather than prolonged periods of ATP depletion. It is possible that dialysis of ATP-depleted oocytes with patch pipette solutions washes out factors required for maintaining channel activity.

Metabolic inhibition leads to swelling in many cell types (e.g., Kimelberg, 1995; Wright and Rees, 1998). We monitored oocyte volume during incubation with metabolic inhibitors by differential interference contrast (DIC) microscopy. Mean ± SE relative cell volume in oocytes exposed to 2-DG and rotenone was 1.01 ± 0.01 (n = 4) just prior to obtaining whole-cell access. The absence of significant cell volume change indicates that channel activation is due to ATP depletion per se rather than secondary oocyte swelling.

The inward current in ATP-depleted oocytes was activated further by strong hyperpolarization (Fig. 1 A). Time-dependent activation of the current by hyperpolarization was fit by a biexponential function describing fast and slow components. The mean ± SE time constants for hyperpolarization-induced current activation at –120 mV were 255 ± 16 and 28 ± 3 ms (Table I). Addition of 10 mM Zn^{2+} to the bath medium inhibited the current by 86 ± 1% (Table I).

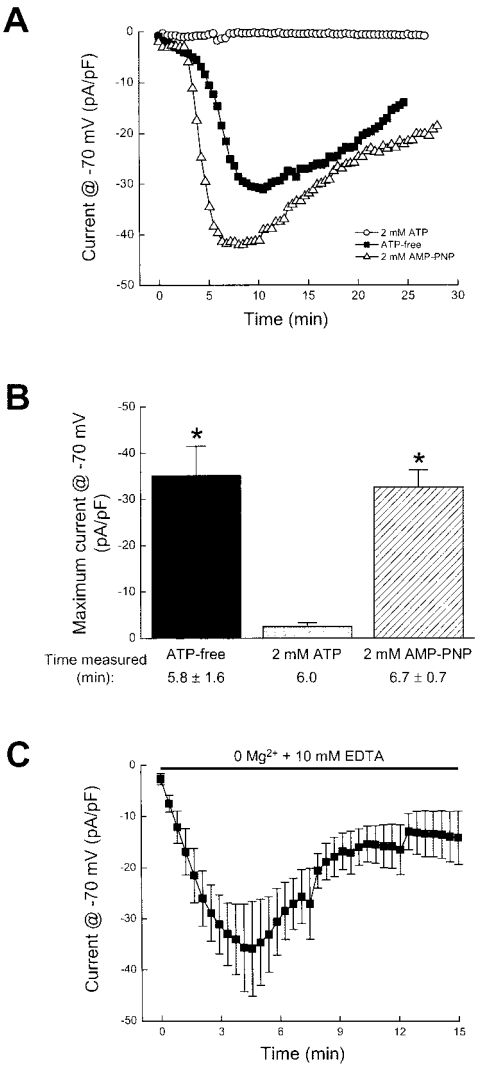

Figure 2. **Dialysis of oocytes with ATP- or Mg^{2+}-free pipette solutions transiently activates CLH-3.** (A) Time course of change in whole-cell Cl^- current in three oocytes dialyzed with metabolic inhibitors and 2 mM ATP, 2 mM AMP-PNP, or an ATP-free pipette solution. (B) Maximum whole-cell Cl^- current densities observed in metabolically poisoned oocytes dialyzed with ATP-free or ATP-containing pipette solutions. Values are means ± SE (n = 4–6). *$P < 0.001$ compared with oocytes dialyzed with 2 mM ATP. The mean ± SE time after obtaining whole-cell access at which peak currents were measured are shown. Whole-cell current was recorded at 6 min after obtaining whole-cell access in oocytes dialyzed with 2 mM ATP. (C) Time course of current activation in cells dialyzed with Mg^{2+}-free pipette solution. Time zero is the time whole-cell access was obtained. Values are means ± SE (n = 4–7). One oocyte examined showed no current activation during dialysis with Mg^{2+}-free pipette solution and was excluded from the dataset shown here.

The strong inward rectification, voltage dependence, and degree of inhibition by Zn^{2+} of the current are virtually identical to the characteristics of CLH-3 current activated by oocyte swelling and oocyte cell cycle progression described by us previously (Rutledge et al., 2001). To determine directly whether the current observed in metabolically poisoned oocytes was due to the activity of CLH-3, we performed RNA_i experiments. Worms were injected with either buffer, *clh-3* double-stranded RNA (dsRNA) or dsRNA for another ClC channel, CLH-5. Oocytes were patch clamped

Table I. **Characteristics of whole-cell current in metabolically poisoned oocytes isolated from worms injected with buffer or *clh-3* dsRNA**

	Buffer inject control	*clh-3* dsRNA inject
Initial whole-cell current density at –70 mV	−26 ± 8 pA/pF	−2.9 ± 1.0 pA/pF[a]
Voltage sensitivity		
τ_1 @−120 mV	255 ± 16 ms	ND
τ_2 @−120 mV	28 ± 3 ms	ND
% inhibition by 10 mM Zn^{2+}	86 ± 1%	ND

[a]Current is significantly ($P < 0.02$) different compared to that in oocytes isolated from buffer-injected worms.
Oocytes were incubated in egg buffer containing 5 mM DG and 1 mM rotenone for 15–40 min and then patch clamped in NMDG-Cl bath solution containing the same metabolic inhibitors. Values are means ± SE ($n = 4$).

20–24 h after injections. Mean ± SE initial whole-cell current densities in metabolically poisoned oocytes from buffer- and *clh-3* dsRNA-injected worms were –26 ± 8 pA/pF and –2.9 ± 1.0 pA/pF ($n = 4$; $P < 0.02$) at –70 mV, respectively (Table I). The initial current in metabolically poisoned oocytes from dsRNA-injected worms was not significantly ($P > 0.9$) different from that of nonmetabolically poisoned control oocytes. Mean ± SE initial current in metabolically poisoned oocytes from *clh-5* dsRNA-injected worms was –36 ± 5 pA/pF ($n = 3$). This value was not significantly ($P > 0.4$) different from that of buffer-injected worms, demonstrating that the inhibitory effect of *clh-3* dsRNA is specific. Taken together, the results in Fig. 1 and Table I demonstrate clearly that metabolic inhibition activates CLH-3.

To further examine the effect of ATP depletion on CLH-3 activation, we patch clamped oocytes with a pipette solution containing 40 μM oligomycin, 20 μM rotenone, and 5 μM iodoacetate with or without hydrolysable ATP. In the presence of 2 mM ATP, whole-cell Cl^- current remained stable. However, when ATP was removed from the pipette solution or replaced with the nonhydrolyzable ATP analogue, AMP-PNP, whole-cell current activated slowly. The current typically reached a stable level 6 to 7 min after obtaining whole-cell access and then inactivated (Fig. 2 A). Mean ± SE peak current densities in cells dialyzed with 2 mM AMP-PNP or an ATP-free pipette solution were −33 ± 4 and –35 ± 6 pA/pF ($n = 4$ to 5) at –70 mV, respectively (Fig. 2 B). In oocytes dialyzed with 2 mM ATP, mean ± SE whole-cell current density measured 6 min after membrane rupture was –2.5 ± 0.9 pA/pF ($n = 6$) at –70 mV (Fig. 2 B). Whole-cell currents in oocytes dialyzed with AMP-PNP or an ATP-free solution were significantly higher ($P < 0.001$) than those in oocytes dialyzed with ATP.

During dialysis with pipette solutions containing metabolic inhibitors, oocytes shrank slightly. The mean ± SE relative volumes measured 5 min after whole-cell access was obtained on oocytes dialyzed with 2 mM ATP, 2 mM AMP-PNP, or an ATP-free pipette solution were 0.94 ± 0.02, 0.94 ± 0.01, and 0.93 ± 0.03 ($n = 4$ to 5), respectively. These results indicate that current activation in oocytes dialyzed with ATP-free solutions is due to ATP depletion rather than cell swelling.

ATP depletion is expected to decrease net protein phosphorylation by reducing or eliminating kinase activity. To further examine the dependence of CLH-3 activity on kinase function, we dialyzed cells with an Mg^{2+}-free pipette solution containing 10 mM EDTA. Magnesium is an essential cofactor required for kinase activity (Saris et al., 2000). As shown in Fig. 2 C, removal of intracellular Mg^{2+} induced a rapid transient activation of current. The mean ± SE peak current density observed under Mg^{2+}-free conditions was –43 ± 11 pA/pF at –70 mV ($n = 7$). No swelling was observed during dialysis of oocytes with a Mg^{2+}-free pipette solution. Mean ± SE relative cell volume was 0.94 ± 0.01 ($n = 4$) 5 min after obtaining whole-cell access.

Inhibition of serine/threonine phosphatases blocks swelling- and meiotic maturation–induced activation of CLH-3

Protein phosphorylation depends not only on the activity of kinases, but also on protein phosphatase (PP) function. Therefore, we examined the effect of phosphatase inhibitors

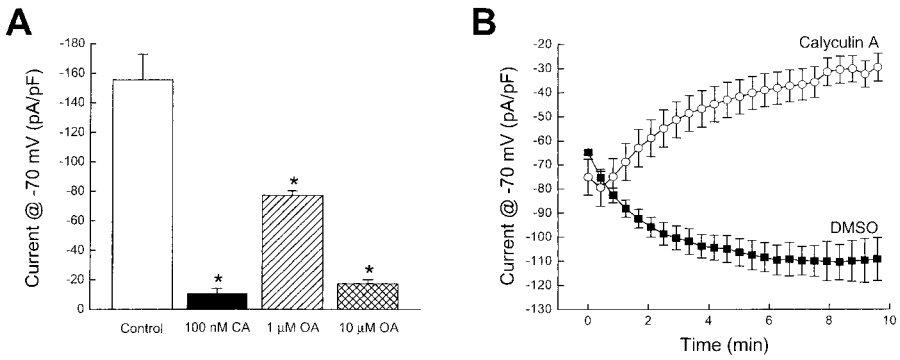

Figure 3. **Serine/threonine phosphatase inhibitors inhibit swelling-induced activation of CLH-3.** (A) Effect of CA and OA on swelling-induced activation of CLH-3. Oocytes were incubated with 100 nM CA in egg buffer for 15–20 min before they were patch clamped and swollen by exposure to hypotonic medium. OA was included in the patch pipette solution. Oocytes were dialyzed with 1 μM OA for 10–13 min or 10 μM OA for 1 min before induction of swelling. Swelling-induced currents were recorded when they had stabilized (8–28 min after exposure of oocytes to hypotonicity). Values are means ± SE ($n = 3$–7). *$P < 0.001$ compared with oocytes exposed to DMSO alone.

on swelling-induced activation of CLH-3 current. Calyculin A (CA) inhibits the serine/threonine phosphatases PP1 and PP2A at nanomolar concentrations (Ishihara et al., 1989). Pretreatment of oocytes with 100 nM CA in the bathing medium for 10–20 min inhibited swelling-induced current activation by >90% ($P < 0.001$; Fig. 3 A). Low concentrations of okadaic acid (OA) inhibit PP2A preferentially, whereas higher concentrations also inhibit PP1 (Cohen et al., 1989; Ishihara et al., 1989). OA had little effect on current activation at concentrations of 100 and 500 nM (unpublished data). However, when oocytes were dialyzed before swelling with patch pipette solutions containing 1 or 10 μM OA, current activation was inhibited ~50 and 90% ($P < 0.001$), respectively (Fig. 3 A).

Addition of CA to the bathing medium also caused rapid inhibition of activated channels. As shown in Fig. 3 B, CLH-3 current was activated to approximately half-maximal levels by swelling, and then 100 nM CA or 0.01% DMSO (control) was added to the bathing medium. In the presence of DMSO, CLH-3 continued to activate and current density reached a mean ± SE steady-state level of 110 ± 15 pA/pF ($n = 3$). Addition of CA to the bath induced an immediate inactivation of the current. Taken together, the results in Figs. 1–3 demonstrate that serine/threonine dephosphorylation events are responsible for activating CLH-3 during cell swelling.

An important physiological signal for activation of CLH-3 in the *C. elegans* oocyte is resumption of the meiotic cell cycle, a process termed meiotic maturation (Rutledge et al., 2001). To determine whether maturation-induced current activation is regulated by protein dephosphorylation, we allowed oocytes to undergo meiotic maturation in vitro. Shortly before maturation begins, the oocyte nucleus increases in size and migrates to the cell periphery (McCarter et al., 1999). Oocytes with centrally located nuclei do not mature after isolation from the gonad. However, when oocytes with off-center nuclei are isolated and placed in a bath chamber, they undergo meiotic maturation (Rutledge et al., 2001). A universal hallmark of maturation is nuclear envelope breakdown (NEBD; also termed germinal vesicle breakdown) (Nebreda and Ferby, 2000).

Fig. 4 A shows maturing oocytes incubated in egg buffer containing 0.01% DMSO or 0.01% DMSO with 100 nM CA. The mean ± SE time after isolation at which NEBD was observed in control and CA-treated oocytes was 6.0 ± 1.5 min ($n = 4$) and 11.3 ± 2.4 min ($n = 3$), respectively. These times are not significantly ($P > 0.1$) different suggesting that CA does not disrupt events associated with initiation of NEBD.

Oocytes were patch clamped after NEBD had begun. CLH-3 in oocytes treated with DMSO alone was constitutively active upon obtaining whole-cell access. Current continued to activate slowly reaching a mean ± SE maximum value of –40 ± 7 pA/pF ($n = 8$) at –70 mV 7-10 min after obtaining whole-cell access. The peak current was stable for 1-3 min and then underwent slow inactivation (Fig. 4 B). No current activation was detected in maturing oocytes treated with 100 nM CA (Fig. 4, B and C). The mean ± SE current density observed 20–22 min after recordings were initiated was –3.0 ± 1.0 pA/pF ($n = 4$). This value was not significantly ($P > 0.2$) different from that observed in nonmaturing oocytes.

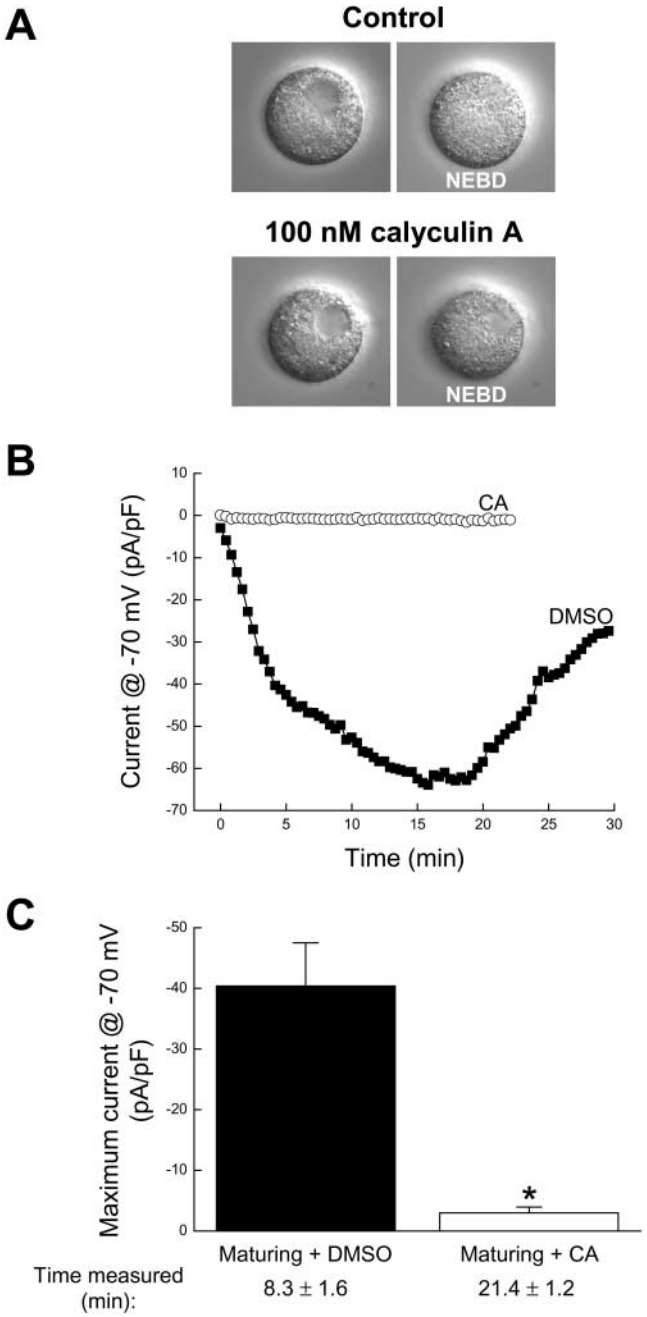

Figure 4. **Meitoic maturation-induced activation of CLH-3 is blocked by the serine/threonine phosphatase inhibitor CA.** (A) DIC micrographs showing in vitro maturation of oocytes incubated in control egg buffer containing 0.01% DMSO and in egg buffer containing 0.01% DMSO and 100 nM CA. (B) Examples of meiotic maturation-induced activation of CLH-3 current in a control oocyte and an oocyte incubated with 100 nM CA. (B) Maximum whole-cell Cl^- current densities observed in oocytes undergoing meiotic maturation in the presence of DMSO or 100 nM CA. Values are means ± SE ($n = 4$–8). *$P < 0.005$ compared with oocytes exposed to DMSO alone.

The type 1 protein phosphatases CeGLC-7α and β mediate swelling- and maturation-induced activation of CLH-3

The lower sensitivity of CLH-3 activation to OA versus CA (Fig. 3) suggests that PP1-type phosphatases function in

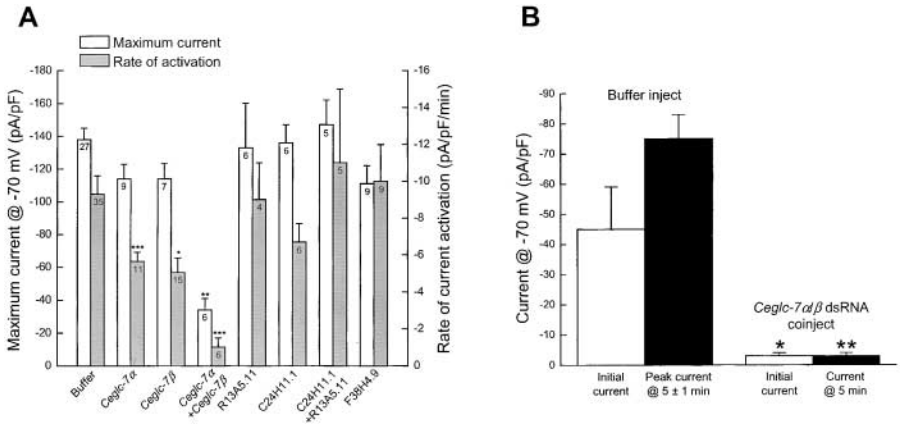

Figure 5. **CLH-3 is regulated by the PP1-type phosphatases CeGLC-7α and CeGLC-7β.** (A) Effects of buffer injections or injection of various dsRNAs on the rate of CLH-3 activation and maximum steady-state current triggered by oocyte swelling. Rates of oocyte swelling were unaffected by dsRNA injections (unpublished data). Values are means ± SE Numbers of oocytes recorded from are shown in each bar. *P < 0.05, **P < 0.01, ***P < 0.001 compared with oocytes from buffer-injected worms. (B) Effects of buffer injection or coinjection of *Ceglc-7α* and *Ceglc-7β* dsRNAs on CLH-3 current activated during oocyte meiotic maturation. Values are means ± SE ($n = 4$). All injections were performed at least two separate times. Buffer injections were performed in parallel with all dsRNA injections. *P < 0.02, **P < 0.0001 compared with oocytes from buffer-injected worms. Injection of *Ceglc-7α*, *Ceglc-7β*, F38H4.9 dsRNAs, or coinjection of *Ceglc-7α/β* dsRNAs caused embryonic lethality as described (Sieburth et al., 1999; Hsu et al., 2000; Piano et al., 2000).

channel regulation (Cohen et al., 1989; Ishihara et al., 1989). The Proteome BioKnowledge® Library (https://www.incyte.com/proteome/mainmenu.jsp) identifies the presence of 38 predicted genes in the *C. elegans* genome that encode PP1-related proteins. Transcripts for four of these genes, *Ceglc-7α* (F29F11.6), *Ceglc-7β* (F56C9.1), C24H11.1, and R13A5.11, have been detected in *C. elegans* oocytes by microarray analyses (Hill et al., 2000). CeGLC7α/β are 85 and 91% identical, respectively, to human PP1α, and have been shown recently to play important roles in *C. elegans* meiotic and mitotic cell cycle events (Hsu et al., 2000; Kaitna et al., 2002; Rogers et al., 2002). C24H11.1 shares 49% identity with human PP1β, and R13A5.11 shares 43% identity with human PP1α. We tested the effect of knockdown of these four PP1-encoding genes on CLH-3 activation using RNA_i. We also examined the effect of RNA_i of F38H4.9, which encodes the single predicted PP2A catalytic subunit in the *C. elegans* genome.

Fig. 5 A shows the rates of swelling-induced CLH-3 activation and maximum currents observed in oocytes from buffer- or dsRNA-injected worms. Knockdown of C24H11.1, R13A5.11, or F38H4.9 had no significant (P > 0.05) effect on channel activation. However, disruption of *Ceglc-7α* and *Ceglc-7β* expression reduced significantly (P < 0.05) the rate of CLH-3 activation by 40–50%.

The partial inhibitory effect of *Ceglc-7α* and *β* suggests that the two phosphatases may have complementary roles and dephosphorylate common substrates as proposed recently for the regulation of *C. elegans* histone H3 phosphorylation (Hsu et al., 2000). Therefore, we examined the effect of coinjection of *Ceglc-7α/β* dsRNAs on CLH-3 activity. As shown in Fig. 5 A, the rate of swelling-induced current activation and maximum current were inhibited by ~90 and 75% (P < 0.01), respectively, in oocytes isolated from coinjected worms. In contrast, coinjection of C24H11.1 and R13A5.11 dsRNAs did not alter current activation. This result indicates that inhibition of CLH-3 by *Ceglc-7α/β* RNA_i is not due to nonspecific effects of coinjection of multiple dsRNA species.

As discussed earlier, an important signal for activation of CLH-3 in vivo is meiotic cell cycle progression. To determine whether CeGLC-7α and β regulate maturation-induced channel activation, we isolated oocytes with off-center nuclei from buffer-injected and *Ceglc-7α/β* dsRNA-coinjected worms and allowed them to undergo meiotic maturation *in vitro*. Mean ± SE initial whole-cell current density was –45 ± 14 pA/pF in maturing oocytes from buffer-injected worms. The current continued to activate during patch clamp recording and reached a maximum level of –75 ± 8 pA/pF 5 ± 1 min ($n = 4$) after obtaining whole-cell access.

NEBD appeared to progress normally in vitro when oocytes with off-center nuclei were isolated from *Ceglc-7α/β* dsRNA coinjected worms. However, activation of CLH-3 was suppressed dramatically by knockdown of the two phosphatases (Fig. 5 B). The initial whole-cell current density and current density measured 5 min after obtaining whole-cell access in oocytes from dsRNA coinjected worms were not significantly (P > 0.9) different from that measured in nonmaturing oocytes (compare Figs. 1 C and 5 B). Mean ± SE whole-cell current density measured 14–36 min after obtaining whole-cell access was –12 ± 4 pA/pF ($n = 4$).

Taken together, the results in Fig. 5 demonstrate that CeGLC-7α and β function in the signaling pathways that activate CLH-3 during cell swelling and meiotic cell cycle progression. The simplest interpretation of the data is that the two phosphatases are capable of dephosphorylating one or more common substrates that regulate channel activation. Alternatively, CLH-3 may be regulated by parallel signaling pathways in which CeGLC-7α and β function independently from one another.

ClC-2 activity is regulated by serine/threonine phosphorylation and dephosphorylation

Human T84 intestinal cells express a volume-sensitive ClC-2-like current that is activated by ATP depletion. In addition, swelling-induced activation of the current is inhibited by CA and also by higher concentrations of OA (Fritsch and Edelman, 1997). Given the similarity of these results to our findings with CLH-3, we wanted to determine directly if ClC-2 is regulated by phosphorylation and dephosphorylation events. HEK293 cells were transiently transfected with

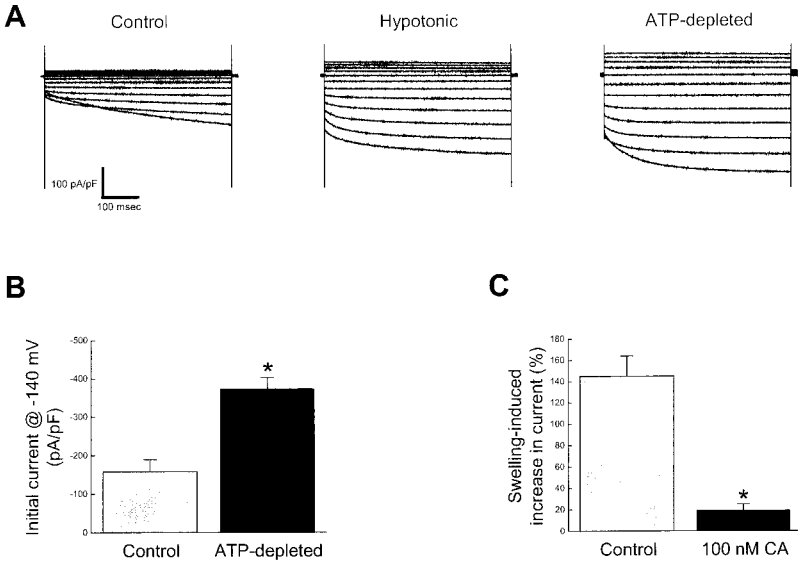

Figure 6. **ClC-2 is activated by protein dephosphorylation events.** (A) Examples of whole-cell currents observed a cell exposed to metabolic inhibitors and dialyzed with an ATP-free pipette solution (ATP-depleted) and in a separate cell under isotonic conditions (Control) and 1 min after cell swelling (Hypotonic). Membrane potential was held at –50 mV. Step changes in whole-cell currents were elicited by stepping membrane voltage from −140 mV to +80 mV in 20 mV steps from a starting potential of 0 mV. Currents were normalized to cell capacitance for comparison. (B) Chloride current densities observed immediately after obtaining the whole-cell configuration in control HEK293 cells or cells exposed to metabolic inhibitors and an ATP-free pipette solution. Values are means ± SE (n = 6–9). *P < 0.0003 compared with control cells treated with DMSO alone. (C) Percent swelling-induced increase in whole-cell Cl^- current density in control cells and cells exposed to 100 nM CA. Steady-state currents were measured at –140 mV. Values are means ± SE (n = 6–7). *P < 0.0001 compared with control cells treated with DMSO alone.

GFP cDNA alone or with a combination of GFP and rat ClC-2 cDNAs. GFP-expressing cells showed no ClC-2 activity under basal conditions or after cell swelling (unpublished data). However, cells expressing ClC-2 exhibited robust inwardly rectifying Cl^- currents that were activated by strong hyperpolarization (Fig. 6 A). Mean steady-state whole-cell Cl^- current density at –140 mV was –158 ± 31 pA/pF (n = 9) in ClC-2–transfected cells.

HEK293 cells were ATP depleted by exposure to 5 mM 2-DG and 1 μM rotenone for 15–25 min and then patch clamped with an ATP-free pipette solution containing 40 μM oligomycin, 20 μM rotenone, and 5 μM iodoacetate. Mean ± SE steady-state current density observed immediately after obtaining the whole-cell configuration was –373 ± 29 pA/pF (n = 6) at –140 mV. This value is approximately 2.5-fold higher than that observed in control cells (Fig. 6 B).

When ClC-2–transfected HEK293 cells were swollen, we observed a rapid increase in ClC-2 current. However, with long periods of cell swelling, the ubiquitous, outwardly rectifying chloride current ($I_{Cl,swell}$) (Strange et al., 1996; Nilius et al., 1997; Okada, 1997) was activated (unpublished data). To avoid contamination of current traces with $I_{Cl,swell}$, we quantified ClC-2 current 1 min after exposure of cells to hypotonic bath medium. This brief period of cell swelling increased whole-cell current density at –140 mV from a mean initial value of –191 ± 46 pA/pF to –409 ± 61 pA/pF (n = 3). When cells were exposed to a bath solution containing 100 nM CA for 6–15 min and then patch clamped with a pipette solution also containing 100 nM CA, swelling-induced current was inhibited >85% (Fig. 6 C). Taken together, the data in Fig. 6 demonstrate that activation of ClC-2 is regulated by serine/threonine dephosphorylation.

Discussion

ClC channels function in organisms as diverse as bacteria, plants, and vertebrate animals. In humans, mutations in four ClC genes give rise to muscle, kidney, and bone disorders (George et al., 2001; Jentsch et al., 2002). Despite their obvious physiological importance, relatively little is known about how ClC channels are regulated. The studies presented here demonstrate clearly that the *C. elegans* ClC channel, CLH-3, is activated by serine/threonine dephosphorylation events during oocyte meiotic maturation and in response to oocyte swelling. Dephosphorylation is mediated by the PP1 orthologues CeGLC-7α and β. The target of these phosphatases is unknown, but may include the channel itself and/or associated regulatory proteins.

Regulation of ClC channels by phosphorylation events

Phosphorylation events have been shown previously to regulate various ClC channel types, but the signaling pathways involved and the physiological context under which this regulation might occur are unknown. For example, human ClC-1 heterologously expressed in HEK293 cells is inhibited by protein kinase C activation (Rosenbohm et al., 1999). Similarly, ClC-1–like Cl^- currents in mouse muscle fibers are activated by staurosporine, a broadly selective protein kinase inhibitor (Chen and Jockusch, 1999). Dialysis of cells patch clamped in the whole-cell mode with autonomously active calcium/calmodulin-dependent protein kinase II activates heterologously expressed human ClC-3 (Huang et al., 2001). Guinea pig ClC-3 is inhibited by protein kinase C– or A-dependent phosphorylation of the channel protein (Duan et al., 1999; Nagasaki et al., 2000).

Phosphorylation events also play a role in regulation of ClC-2. For example, a native ClC-2–like current in T84 cells is activated by intracellular ATP depletion (Fritsch and Edelman, 1996). Swelling-induced activation of the current is inhibited by CA and higher concentrations of okadiac acid suggesting that a PP1 functions in channel regulation (Fritsch and Edelman, 1997). These results are strikingly similar to our findings on CLH-3 (Figs. 1–3) as well as heterologously expressed rat ClC-2 (Fig. 6).

Ascidian embryos express a swelling- and hyperpolarization-activated inwardly rectifying Cl^- current with biophysical properties similar to those of CLH-3 and ClC-2. The physiological functions and molecular identity of the ascidian channel are unknown, but current levels increase nearly tenfold during entry into M-phase of the mitotic cell cycle (Block and Moody, 1990; Coombs, et al., 1992). An inhibitor of cell cycle–dependent kinases, 6-dimethylaminopurine, increases current amplitude suggesting that, like CLH-3, the channel is activated by protein dephosphorylation events (Villaz et al., 1995).

Recently, Furukawa et al. (2002) demonstrated that rabbit ClC-2 is phosphorylated at serine 632 by the M-phase specific cyclin-dependent kinase (CDK) p34cdc2/cyclin B. Serine 632 is located within a CDK phosphorylation consensus site on the COOH terminus of the channel. Phosphorylation of serine 632 dramatically inhibits ClC-2 activity. CDK phosphorylation consensus sites are present on the COOH terminus of the CLH-3 cDNA cloned by Nehrke and coworkers (Nehrke et al., 2000) suggesting that CDKs may regulate channel activity.

Regulation of CLH-3 and ClC-2 by type 1 protein phosphatases

Type 1 protein phosphatases have been shown to play critical roles in regulating mitotic and meiotic cell cycle events in a variety of organisms (Berndt, 1999; Varmuza et al., 1999; Bollen and Beullens, 2002). Our RNA_i studies demonstrate clearly that dephosphorylation-dependent activation of CLH-3 during oocyte meiotic maturation and in response to oocyte swelling are mediated by the PP1-type phosphatases CeGlC-7α and β (Fig. 5). These phosphatases have been shown previously to play important roles in mitotic and meiotic cell cycle progression in *C. elegans*. Hsu et al. (2000) demonstrated that CeGLC-7α and β function together with the aurora kinase AIR-2 to regulate histone H3 phosphorylation. Regulation of histone phosphorylation in turn plays a critical role in controlling chromosome dynamics during meiotic and mitotic divisions. CeGLC-7α and β have also been shown to directly or indirectly antagonize AIR-2–dependent phosphorylation of the meiotic cohesin REC-8 (Rogers et al., 2002). Alterations in REC-8 function disrupt meiotic chromosome segregation. For example, early separation of sister chromatids at the onset of anaphase I is observed when *Ceglc-7α/β* expression are disrupted by RNA_i. Kaitna et al. (2002) have also observed premature chromatid separation after disruption of *Ceglc-7α/β* expression and have suggested that this effect is dependent on the activity of the SEP-1 separase.

It is interesting to note that Furukawa et al. (2002) demonstrated recently by yeast two-hybrid analyses that rat PP1α and PP1β interact with the COOH terminus of rabbit ClC-2. These two phosphatases share 85–93% amino acid identity with CeGLC-7α and β. Given the critical roles of CeGLC-7α and β in dephosphorylation-dependent activation of CLH-3 and the regulation of ClC-2 function by serine/threonine phosphorylation (Fig. 6; Furukawa et al., 2002), it seems likely that mammalian PP1α and PP1β activate ClC-2 by dephosphorylating the channel and/or associated regulatory proteins.

Are CLH-3 and ClC-2 orthologues?

Orthologues are genes in different species that arose from a common ancestor and that carry out similar physiological roles (Remm et al., 2001). We have suggested previously that CLH-3 and ClC-2 are orthologues (Rutledge et al., 2001; Strange, 2002). The studies described here as well as recent findings on ClC-2 further strengthen this hypothesis. CLH-3 and ClC-2 share 40% amino acid identity, are activated by cell swelling, and have biophysical and pharmacological properties that are strikingly similar (for review by Strange, 2002). ClC-2 is expressed widely in mammalian cells and tissues and mRNA levels are particularly high in the brain, kidney, and intestine (Jentsch et al., 2002). CLH-3 is expressed in the excretory cell (the worm kidney), intestine, hermaphrodite-specific neurons, enteric muscles, uterus (Schriever et al., 1999; Nehrke et al., 2000), and oocytes (Rutledge et al., 2001).

Like CLH-3, ClC-2 is activated by serine/threonine dephosphorylation events that are possibly mediated by type 1 protein phosphatases (Figs. 1–6; Furukawa et al., 2002). Activation of CLH-3 in the *C. elegans* oocyte occurs during meiotic maturation (Fig. 4; Rutledge et al., 2001). In ascidian embryos, a ClC-2–like current is activated during M-phase of mitosis (Block and Moody, 1990; Coombs et al., 1992; Villaz et al., 1995). Heterologously expressed rabbit ClC-2 is inhibited by M-phase–specific CDK-mediated phosphorylation (Furukawa et al., 2002).

ClC-2 has been postulated to carry out a number of physiological functions, including transepithelial transport, cell volume regulation, and regulation of intracellular Cl^- in neurons (George et al., 2001; Jentsch et al., 2002). However, knockout of ClC-2 in mice has no readily apparent gross effect on these physiological processes. Instead, ClC-2 knockout causes the retina and testes to degenerate progressively resulting in blindness and male sterility (Bösl et al., 2001).

C. elegans oocytes are surrounded by and coupled via gap junctions to smooth muscle-like sheath cells (Hall et al., 1999). During meiotic maturation, sheath cells contract forcefully driving the oocyte into the spermatheca where it is fertilized. Ovulatory contractions are triggered by the maturing oocyte (McCarter et al., 1999). Meiotic maturation also triggers activation of CLH-3 via CeGLC-7α/β-mediated protein dephosphorylation (Figs. 4 and 5). We have shown previously that knockdown of CLH-3 expression by RNA_i disrupts the timing of sheath cell ovulatory contractions (Rutledge et al., 2001). We have suggested that channel activation depolarizes the oocyte and gap junction–coupled sheath cells and that depolarization may modulate Ca^{2+} signaling pathways that control sheath contractility (Rutledge et al., 2001; Strange, 2002). Additional studies using a variety of approaches including phosphatase knockdown by RNA_i combined with in vivo measurements of channel activity, membrane potentials, sheath contractility and sheath cell Ca^{2+} signaling are warranted and may shed further light on CLH-3 regulation and its precise physiological function.

What do the *C. elegans* hermaphrodite gonad and mammalian testis and retina have in common? All three organs contain cell types that interact closely with and are functionally dependent upon one another. The worm gonad and seminiferous tubule are reproductive tissues that contain germ

cells critically dependent on the precise timing and functioning of developmental pathways and the meiotic cell cycle. Seminiferous tubules are comprised of Sertoli cells and developing sperm cells. Sertoli cells control development of spermatogonia into spermatozoa by direct, cell–cell physical interaction, by secretion of growth factors and nutrients, and by controlling the ionic environment within the seminiferous tubule lumen (Grandjean et al., 1997; Griswold, 1998). In an analogous fashion, oocytes are coupled to sheath cells via gap junctions and functional interactions between the two cell types is essential for regulating oocyte development, meiotic cell cycle events, and ovulation (Greenstein et al., 1994; Rose et al., 1997; Hall et al., 1999; McCarter et al., 1999).

The vertebrate retina is composed of four main cellular layers that interact closely and communicate with each other. Outer segments of rod and cone photoreceptor cells are in direct contact with and surrounded by the apical membrane of the RPE. This close interaction is essential for photoreceptor function and survival. RPE cells provide nutritional support to photoreceptors and they phagocytose and degrade rhodopsin-containing membrane-bound discs that are shed continually from the tips of these cells (Nguyen-Legros and Hicks, 2000). Bösl et al. (2001) have suggested that ClC-2 may regulate local ionic environments essential for cell survival and function in the seminiferous tubule and retina. However, it is also conceivable that ClC-2 may play a signaling role in these tissues analogous to what we have proposed for CLH-3 in the *C. elegans* gonad (Strange, 2002).

Nematodes are estimated to have diverged from other metazoans 600–1,200 million years ago (Blaxter, 1998). The conservation of the functional properties and primary structure of CLH-3 and ClC-2 over such vast evolutionary distances suggests that the channels may play important roles in conserved cell cycle–dependent physiological processes and heterologous cell–cell interactions and communication. Detailed molecular characterization of CLH-3 function and regulation in nematodes will likely continue to provide unique insights into ClC-2 specifically, and ClC anion channels in general.

Materials and methods

C. elegans strains

The N2 (Bristol) *C. elegans* strain was cultured at 20°C using standard methods (Brenner, 1974).

Isolation of oocytes

Gonads were isolated by placing single nematodes in egg buffer (118 mM NaCl, 48 mM KCl, 2 mM $CaCl_2$, 2 mM $MgCl_2$, 25 mM Hepes, pH 7.3, 340 mOsm) and cutting them behind the pharyngeal bulb and in front of the spermatheca using a 26-gauge needle. Isolated gonads were transferred to a patch clamp bath chamber. Late stage oocytes were spontaneously released from the cut end of the gonad.

Patch clamp recordings and oocyte volume measurements

Oocytes were allowed to attach to the cover slip bottom of a bath chamber mounted onto the stage of an inverted microscope. Patch electrodes were pulled from 1.5-mm outer diameter silanized borosilicate microhematocrit tubes. Currents were measured with an Axopatch 200B (Axon Instruments) patch clamp amplifier using a bath solution containing 116 mM NMDG-Cl, 2 mM $CaCl_2$, 2 mM $MgCl_2$, 25 mM Hepes, and 71 mM sucrose (pH 7.3, 340 mOsm) and a pipette solution containing 116 mM NMDG-Cl, 2 mM $MgSO_4$, 20 mM Hepes, 6 mM CsOH, 1 mM EGTA, 48 mM sucrose, 2 mM ATP, and 0.5 mM GTP (pH 7.2, 315 mOsm). Oocytes were swollen by exposure to a hypotonic (260 mOsm) bath solution that contained no added sucrose. Metabolic and phosphatase inhibitors were dissolved as stock solution in DMSO and then added to pipette or bath solutions at a final DMSO concentration of ≤0.01%.

Electrical connections to the patch clamp amplifier were made using Ag/AgCl wires and 3 M KCl/agar bridges. Data acquisition and analysis were performed using pClamp 8 software (Axon Instruments). Changes in whole-cell current were monitored by ramping membrane potential from −80 to +80 mV at 80 mV/s every 5 s. Whole-cell currents and volume changes were measured simultaneously in single oocytes. Patch-clamped oocytes were visualized by video-enhanced DIC microscopy. Oocytes have a spherical morphology and relative cell volume change was determined as $(\text{experimental CSA}/\text{control CSA})^{3/2}$, where CSA is the cell cross-sectional area measured at a single focal plane located at the point of maximum oocyte diameter. DIC images were recorded by CCD camera on video tape and CSA measured offline by image processing.

RNA interference

dsRNA was synthesized using established methods (Fire et al., 1998). Briefly, DNA templates were obtained by PCR and sense and antisense RNA synthesized by T7 polymerase (MEGAscript; Ambion). Template DNA was digested with DNaseI and RNA was precipitated with 3 M sodium acetate and ethanol. Precipitated RNA was washed with 70% ethanol, air-dried, and dissolved in water. RNA size, purity, and integrity were assayed on agarose gels. dsRNA was formed by annealing sense and antisense RNA at 65 °C for 30 min. Annealed dsRNA was diluted into potassium citrate buffer for injection. Worms were injected in one gonad arm with ~1,000,000 molecules of dsRNA or with a similar volume of potassium citrate buffer. For coinjection studies, worms were injected with ~500,000 molecules of two different dsRNA species. The open reading frame locations of each dsRNA used were as follows: *clh-3*, bp 1-847; *Ceglc-7α*, bp 60-949; *Ceglc-7β*, bp 136-935; R13A5.11, bp 51-745; C24H11.1, bp 417-1118; and F38H4.9, bp 149-850.

Transient expression and patch clamp recording of rat ClC-2

HEK293 (human embryonic kidney) cells were cultured in Eagle's minimal essential medium (MEM; GIBCO BRL) containing 10% heat-inactivated horse serum (GIBCO BRL), 50 U/ml penicillin, and 50 μg/ml streptomycin. Cells grown in 35-mm dishes to ~50% confluency were transfected using LipofectAMINE 2000 (Invitrogen) with either 2 μg GFP cDNA ligated into pcDNA3 or 1 μg GFP cDNA and 1 μg rat ClC-2 cDNA ligated into pFROG. After overnight incubation, the transfection medium was replaced with MEM. Patch clamp experiments were performed 24–48 h after transfection using a bath solution containing 90 mM NMDG-Cl, 5 mM $MgSO_4$, 1 mM $CaCl_2$, 12 mM Hepes, 8 mM Tris, 5 mM glucose, and 2 mM glutamine (pH 7.4, 295 mOsm), and a pipette solution containing 116 mM NMDG-Cl, 2 mM $MgSO_4$, 20 mM Hepes, 6 mM CsOH, 1 mM EGTA, 2 mM ATP, 0.5 mM GTP, and 10 mM sucrose (pH 7.2, 275 mOsm). Cells were swollen by exposure to a hypotonic (225 mOsm) bath solution that contained no added sucrose.

Statistical analyses

Data are presented as means ± SE. Statistical significance was determined using Student's two-tailed *t* test for unpaired means or analysis of variance with a Tukey post test. P values of ≤0.05 were taken to indicate statistical significance.

We thank Dr. Thomas Jentsch (University of Hamburg, Hamburg, Germany) for the gift of rat ClC-2 cDNA.

This work was supported by National Institutes of Health grants R01 DK61168 and DK51610, by National Institutes of Health National Research Service Award F32 GM20764 to E. Rutledge, and by National Institutes of Health training grant T32 NS07491 to J. Denton.

References

Berndt, N. 1999. Protein dephosphorylation and the intracellular control of the cell number. *Front. Biosci.* 4:D22–D42.

Blaxter, M. 1998. *Caenorhabditis elegans* is a nematode. *Science.* 282:2041–2046.

Block, M.L., and W.J. Moody. 1990. A voltage-dependent chloride current linked to the cell cycle in ascidian embryos. *Science.* 247:1090–1092.

Bollen, M., and M. Beullens. 2002. Signaling by protein phosphatases in the nucleus. *Trends Cell Biol.* 12:138–145.

Bösl, M.R., V. Stein, C. Hubner, A.A. Zdebik, S.E. Jordt, A.K. Mukhopadhyay, M.S. Davidoff, A.F. Holstein, and T.J. Jentsch. 2001. Male germ cells and photoreceptors, both dependent on close cell-cell interactions, degenerate upon ClC-2 Cl^- channel disruption. *EMBO J.* 20:1289–1299.

Brenner, S. 1974. The genetics of *Caenorhabditis elegans. Genetics.* 77:71–94.

Chen, M.F., and H. Jockusch. 1999. Role of phosphorylation and physiological state in the regulation of the muscular chloride channel ClC-1: a voltage-clamp study on isolated *M. interosseus* fibers. *Biochem. Biophys. Res. Commun.* 261:528–533.

Cohen, P., S. Klumpp, and D.L. Schelling. 1989. An improved procedure for identifying and quantitating protein phosphatases in mammalian tissues. *FEBS Lett.* 250:596–600.

Coombs, J.L., M. Villaz, and W.J. Moody. 1992. Changes in voltage-dependent ion currents during meiosis and first mitosis in eggs of an ascidian. *Dev. Biol.* 153:272–282.

Duan, D., S. Cowley, B. Horowitz, and J.R. Hume. 1999. A serine residue in ClC-3 links phosphorylation-dephosphorylation to chloride channel regulation by cell volume. *J. Gen. Physiol.* 113:57–70.

Dutzler, R., E.B. Campbell, M. Cadene, B.T. Chait, and R. MacKinnon. 2002. X-ray structure of a ClC chloride channel at 3.0 Å reveals the molecular basis of anion selectivity. *Nature.* 415:287–294.

Ferrell, J.E.J. 1999. *Xenopus* oocyte maturation: new lessons from a good egg. *Bioessays.* 21:833–842.

Fire, A., S. Xu, M.K. Montgomery, S.A. Kostas, S.E. Driver, and C.C. Mello. 1998. Potent and specific genetic interference by double-stranded RNA in *Caenorhabditis elegans. Nature.* 391:806–811.

Frings, S., D. Reuter, and S.J. Kleene. 2000. Neuronal Ca^{2+}-activated Cl^- channels–homing in on an elusive channel species. *Prog. Neurobiol.* 60:247–289.

Fritsch, J., and A. Edelman. 1996. Modulation of the hyperpolarization-activated Cl^- current in human intestinal T84 epithelial cells by phosphorylation. *J. Physiol.* 490:115–128.

Fritsch, J., and A. Edelman. 1997. Osmosensitivity of the hyperpolarization-activated chloride current in human intestinal T84 cells. *Am. J. Physiol.* 272: C778–C786.

Furukawa, T., T. Ogura, Y.-J. Zheng, H. Tsuchiya, H. Nakaya, Y. Katayama, and N. Inagaki. 2002. Phosphorylation and functional regulation of ClC-2 chloride channels expressed in *Xenopus* oocytes by M cyclin-dependent protein kinase. *J. Physiol.* 540:883–899.

George, A.L., Jr., L. Bianchi, E.M. Link, and C.G. Vanoye. 2001. From stones to bones: The biology of ClC chloride channels. *Curr. Biol.* 11:R620–R628.

Grandjean, V., J. Sage, F. Ranc, F. Cuzin, and M. Rassoulzadegan. 1997. Stage-specific signals in germ line differentiation: control of Sertoli cell phagocytic activity by spermatogenic cells. *Dev. Biol.* 184:165–174.

Greenstein, D., S. Hird, R.H. Plasterk, Y. Andachi, Y. Kohara, B. Wang, M. Finney, and G. Ruvkun. 1994. Targeted mutations in the *Caenorhabditis elegans* POU homeo box gene *ceh-18* cause defects in oocyte cell cycle arrest, gonad migration, and epidermal differentiation. *Genes Dev.* 8:1935–1948.

Griswold, M.D. 1998. The central role of Sertoli cells in spermatogenesis. *Semin. Cell Dev. Biol.* 9:411–416.

Gulbins, E., A. Jekle, K. Ferlinz, H. Grassme, and F. Lang. 2000. Physiology of apoptosis. *Am. J. Physiol.* 279:F605–F615.

Hall, D.H., V.P. Winfrey, G. Blaeuer, L.H. Hoffman, T. Furuta, K.L. Rose, O. Hobert, and D. Greenstein. 1999. Ultrastructural features of the adult hermaphrodite gonad of *Caenorhabditis elegans*: relations between the germ line and soma. *Dev. Biol.* 212:101–123.

Hill, A.A., C.P. Hunter, B.T. Tsung, G. Tucker-Kellogg, and E.L. Brown. 2000. Genomic analysis of gene expression in *C. elegans. Science.* 290:809–812.

Hsu, J.Y., Z.W. Sun, X. Li, M. Reuben, K. Tatchell, D.K. Bishop, J.M. Grushcow, C.J. Brame, J.A. Caldwell, D.F. Hunt, et al. 2000. Mitotic phosphorylation of histone H3 is governed by Ipl1/aurora kinase and Glc7/PP1 phosphatase in budding yeast and nematodes. *Cell.* 102:279–291.

Huang, P., J. Liu, A. Di, N.C. Robinson, M.W. Musch, M.A. Kaetzel, and D.J. Nelson. 2001. Regulation of human CLC-3 channels by multifunctional Ca^{2+}/calmodulin-dependent protein kinase. *J. Biol. Chem.* 276:20093–20100.

Ishihara, H., B.L. Martin, D.L. Brautigan, H. Karaki, H. Ozaki, Y. Kato, N. Fusetani, S. Watabe, K. Hashimoto, and D. Uemura. 1989. Calyculin A and okadaic acid: inhibitors of protein phosphatase activity. *Biochem. Biophys. Res. Commun.* 159:871–877.

Jentsch, T.J., V. Stein, F. Weinreich, and A.A. Zdebik. 2002. Molecular structure and physiological function of chloride channels. *Physiol. Rev.* 82:503–568.

Kaitna, S., P. Pasierbek, M. Jantsch, J. Loidl, and M. Glotzer. 2002. The aurora B kinase AIR-2 regulates kinetochores during mitosis and is required for separation of homologous chromosomes during meiosis. *Curr. Biol.* 12:798–812.

Kimelberg, H.K. 1995. Current concepts of brain edema. *J. Neurosurg.* 83:1051–1059.

Maduke, M., C. Miller, and J.A. Mindell. 2000. A decade of CLC chloride channels: structure, mechanism, and many unsettled questions. *Annu. Rev. Biophys. Biomol. Struct.* 29:411–438.

McCarter, J., B. Bartlett, T. Dang, and T. Schedl. 1999. On the control of oocyte meiotic maturation and ovulation in *Caenorhabditis elegans. Dev. Biol.* 205: 111–128.

Morgan, D.O. 1997. Cyclin-dependent kinases: engines, clocks, and microprocessors. *Annu. Rev. Cell Dev. Biol.* 13:261–291.

Nagasaki, M., L. Ye, D. Duan, B. Horowitz, and J.R. Hume. 2000. Intracellular cyclic AMP inhibits native and recombinant volume-regulated chloride channels from mammalian heart. *J. Physiol.* 523:705–717.

Nebreda, A.R., and I. Ferby. 2000. Regulation of the meiotic cell cycle in oocytes. *Curr. Opin. Cell Biol.* 12:666–675.

Nehrke, K., T. Begenisich, J. Pilato, and J.E. Melvin. 2000. *C. elegans* ClC-type chloride channels: novel variants and functional expression. *Am. J. Physiol.* 279:C2052–C2066.

Nilius, B., J. Eggermont, T. Voets, G. Buyse, V. Manolopoulos, and G. Droogmans. 1997. Properties of volume-regulated anion channels in mammalian cells. *Prog. Biophys. Mol. Biol.* 68:69–119.

Nguyen-Legros, J., and D. Hicks. 2000. Renewal of photoreceptor outer segments and their phagocytosis by the retinal pigment epithelium. *Int. Rev. Cytol.* 196:245–313.

Okada, Y. 1997. Volume expansion-sensing outward-rectifier Cl^- channel: fresh start to the molecular identity and volume sensor. *Am. J. Physiol.* 273:C755–C789.

Petalcorin, M.I., T. Oka, M. Koga, K. Ogura, Y. Wada, Y. Ohshima, and M. Futai. 1999. Disruption of clh-1, a chloride channel gene, results in a wider body of *Caenorhabditis elegans. J. Mol. Biol.* 294:347–355.

Piano, F., A.J. Schetterdagger, M. Mangone, L. Stein, and K.J. Kemphues. 2000. RNAi analysis of genes expressed in the ovary of *Caenorhabditis elegans. Curr. Biol.* 10:1619–1622.

Remm, M., C.E. Storm, and E.L. Sonnhammer. 2001. Automatic clustering of orthologs and in-paralogs from pairwise species comparisons. *J. Mol. Biol.* 314:1041–1052.

Rogers, E., J.D. Bishop, J.A. Waddle, J.M. Schumacher, and R. Lin. 2002. The aurora kinase AIR-2 functions in the release of chromosome cohesion in *Caenorhabditis elegans* meiosis. *J. Cell Biol.* 157:219–229.

Rose, K.L., V.P. Winfrey, L.H. Hoffman, D.H. Hall, T. Furuta, and D. Greenstein. 1997. The POU gene ceh-18 promotes gonadal sheath cell differentiation and function required for meiotic maturation and ovulation in *Caenorhabditis elegans. Dev. Biol.* 192:59–77.

Rosenbohm, A., R. Rudel, and C. Fahlke. 1999. Regulation of the human skeletal muscle chloride channel hClC-1 by protein kinase C. *J. Physiol.* 514:677–685.

Rutledge, E., L. Bianchi, M. Christensen, C. Boehmer, R. Morrison, A. Broslat, A.M. Beld, A. George, D. Greenstein, and K. Strange. 2001. CLH-3, a ClC-2 anion channel ortholog activated during meiotic maturation in *C. elegans* oocytes. *Curr. Biol.* 11:161–170.

Saris, N.E., E. Mervaala, H. Karppanen, J.A. Khawaja, and A. Lewenstam. 2000. Magnesium. An update on physiological, clinical and analytical aspects. *Clin. Chim. Acta.* 294:1–26.

Schriever, A.M., T. Friedrich, M. Pusch, and T.J. Jentsch. 1999. CLC chloride channels in *Caenorhabditis elegans. J. Biol. Chem.* 274:34238–34244.

Sieburth, D.S., M. Sundaram, R.M. Howard, and M. Han. 1999. A PP2A regulatory subunit positively regulates Ras-mediated signaling during *Caenorhabditis elegans* vulval induction. *Genes Dev.* 13:2562–2569.

Strange, K. 2002. Of mice and worms: novel insights into ClC-2 anion channel physiology. *News Physiol. Sci.* 17:11–16.

Strange, K., F. Emma, and P.S. Jackson. 1996. Cellular and molecular physiology of volume-sensitive anion channels. *Am. J. Physiol.* 270:C711–C730.

Varmuza, S., A. Jurisicova, K. Okano, J. Hudson, K. Boekelheide, and E.B. Shipp. 1999. Spermiogenesis is impaired in mice bearing a targeted mutation in the protein phosphatase 1cγ gene. *Dev. Biol.* 205:98–110.

Villaz, M., J.C. Cinniger, and W.J. Moody. 1995. A voltage-gated chloride channel in ascidian embryos modulated by both the cell cycle clock and cell volume. *J. Physiol.* 488:689–699.

Wondergem, R., W. Gong, S.H. Monen, S.N. Dooley, J.L. Gonce, T.D. Conner, M. Houser, T.W. Ecay, and K.E. Ferslew. 2001. Blocking swelling-activated chloride current inhibits mouse liver cell proliferation. *J. Physiol.* 532:661–672.

Wright, A.R., and S.A. Rees. 1998. Cardiac cell volume: crystal clear or murky waters? A comparison with other cell types. *Pharmacol. Ther.* 80:89–121.